Internal and external forcing of sea level variability in the Black Sea

Denis L. Volkov[1] and Felix W. Landerer[2]

[1]Cooperative Institute for Marine and Atmospheric Studies, University of Miami, and Atlantic Oceanographic and Meteorological Laboratory, NOAA, Miami, Florida
[2]Jet Propulsion Laboratory, California Institute of Technology, Pasadena, California

contact: denis.volkov@noaa.gov

UNIVERSITY OF MIAMI

1. Overview

Project goal:

This project – funded through NASA's *Ocean-Surface-Topography Science Team* – seeks to investigate the following:

1. What caused the extreme sea level increase in 2010 and 2011 in the Mediterranean and Black seas, as well as similar events in the past?
2. What's the relative contribution of steric and non-steric components to the sea level budget on monthly to interannual time-scales?
3. What are contributions to sea level changes by mass flow through the Strait of Gibraltar, fresh water fluxes, and steric effects?
4. What's the relationship between the atmospheric circulation over the subtropical North Atlantic, sea level to the west of the Strait of Gibraltar, and sea level in the Mediterranean Sea?
5. What's the statistical and dynamical relationship between the sea level in the Eastern Mediterranean and in the Black Sea?

Approach:

We use an array of observing systems that monitor [1] the sea surface height (SSH; from altimetry & tide- gauges), [2] time-varying gravity from GRACE (JPL-RL05 Mascons), [3] hydrographic properties (temperature and salinity records; Argo etc.), and [4] ocean surface wind (QuikSCAT, ASCAT, etc.). To assess the sensitivity of sea level in the Mediterranean and Black Sea region, complement our analysis of the observations with atmospheric reanalysis (e.g. ERA-Interim), and ocean model simulations (e.g., ECCO2 project).

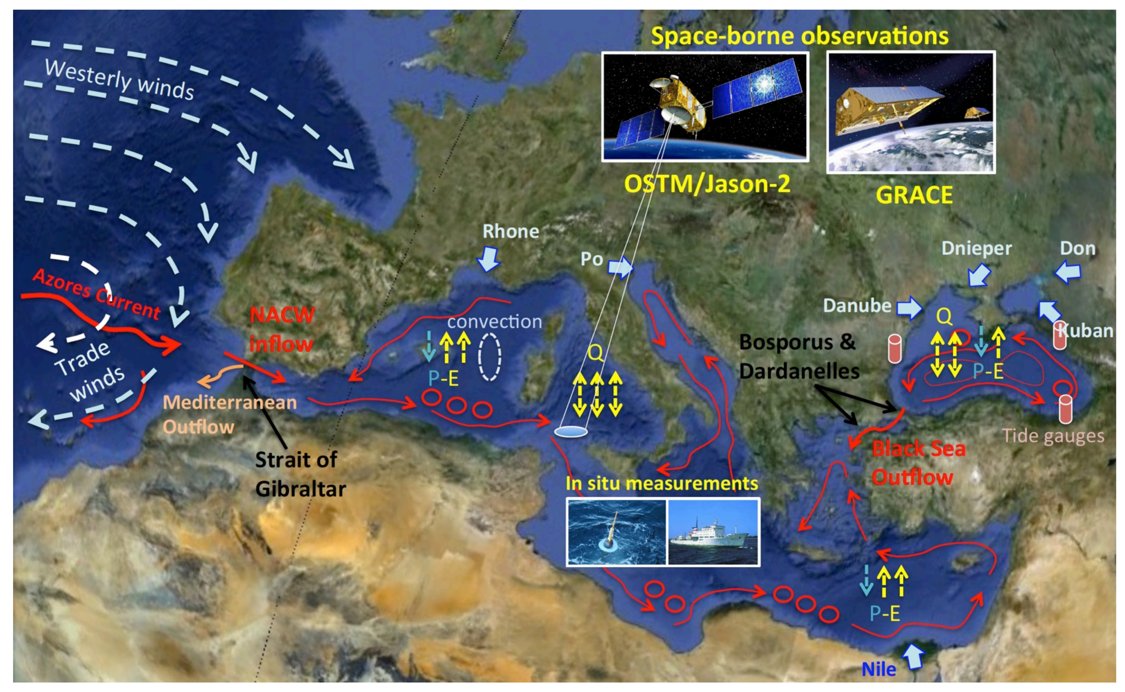

Fig.1 Schematic illustrating the main physical processes driving sea level variability in the Mediterranean and Black Seas. NACW – North Atlantic Central Water, Q – net surface heat flux, P-E means Precipitation-Evaporation. Red arrows show near-surface circulation.

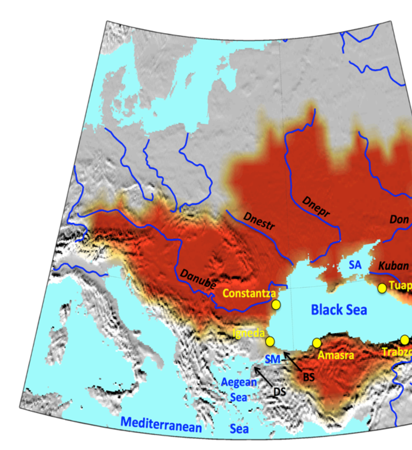

Fig.2 Land area that drains into the Black Sea. The largest river Danube contributes 205 km^3/yr, followed by the Dnepr with 47 km^3/yr. The total annual discharge is approx. 350 km^3/yr.

2. Summary

1. Satellite altimetry and tide gauges have observed strong fluctuations of SLA in the Black Sea with very high anomalies in February 2010, January 2011, and April 2013 **[-> Fig. 3].**
2. Seasonal cycle of sea level in Black Sea is smaller than in Mediterranean; variability is dominated by the non-seasonal signals **[-> Fig. 4].**
3. Seasonal sea level budget shows comparable contributions of precipitation and evaporation over the Black Sea (internal processes), river discharge and outflow (external processes); impact of surface heat flux (internal process) is rather small **[-> Fig. 5]**.
4. Non-seasonal sea level in the Black and in the Aegean seas are correlated; the Black Sea lags behind the Aegean Sea by 1 month, suggesting influence of external dynamic processes on Black Sea sea level **[-> Fig. 3].**
5. GRACE observations can be used to study interannual variability of river discharge into the Black Sea, but ERA-I reanalysis biases exist **[-> Fig. 6].**
6. Non-seasonal sea level budget is dominated by freshwater fluxes; external processes such as river discharge and changes in outflow likely responsible for large anomalies in February 2010, January 2011, and April 2013 **[-> Fig. 7 & 9]**
7. Strong correlation between non-seasonal SLA in the Black Sea and land water storage over the Black Sea drainage basin, indicating importance of river discharge to the large anomalies **[-> Fig. 7 & 8].**
8. Water storage anomalies over the Black Sea drainage basin are caused by precipitation and evaporation that are dependent on the large-scale atmospheric circulation pattern modulated by the North-Atlantic-Oscillation (NAO) **[-> Fig. 7, 8 & 9].**
9. NAO-related large-scale atmospheric circulation drives the sea level variability over the Mediterranean and Black seas by wind forcing near the Strait of Gibraltar and over the Aegean Sea and Turkish Straits, respectively **[-> Fig. 9].**

3. Results

3.1 Seasonal and non-seasonal Sea Level variations

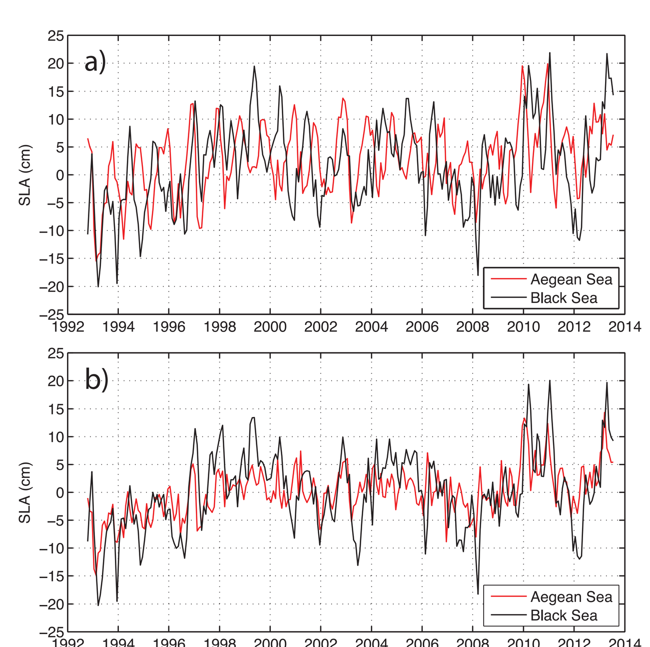

Fig. 3 The time series of SLA averaged over the Black (**black**) and Aegean (**red**) seas: (a) seasonal cycle is present and (b) seasonal cycle is removed. Maximum correlation between the time series in (b) is 0.75 at 1 month time lag.

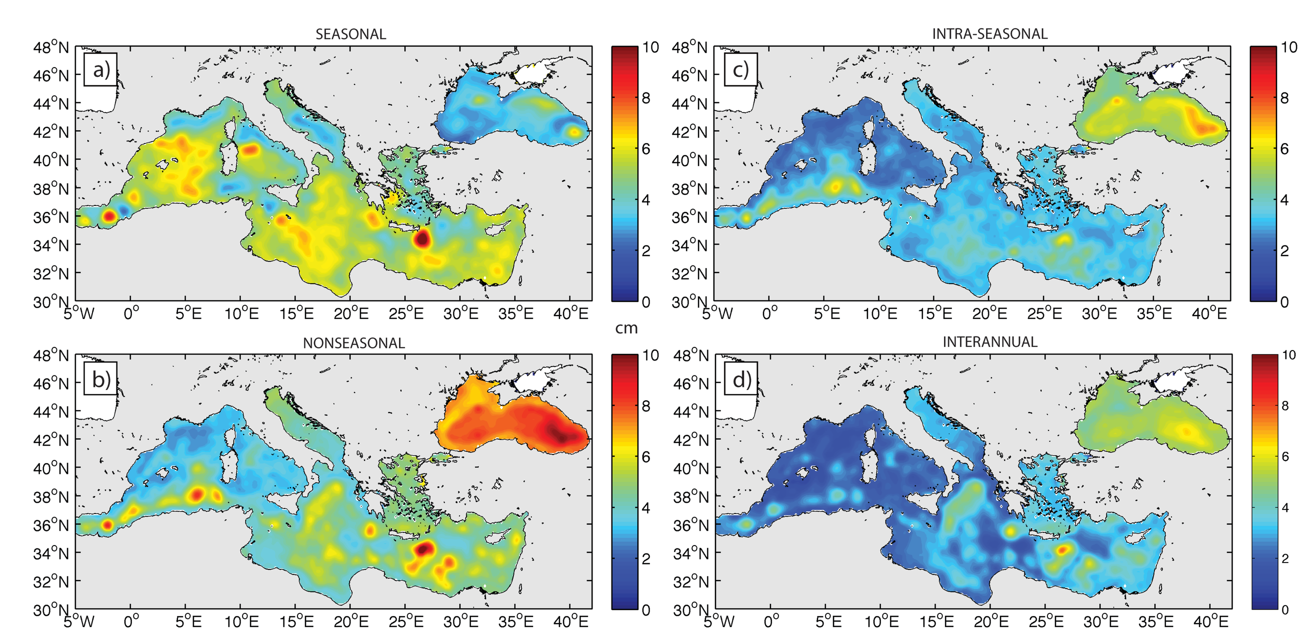

Fig. 4 Standard deviations of sea level: (a) seasonal cycle, (b) non-seasonal variability (after the seasonal cycle has been removed), (c) intra-seasonal signals, and (d) interannual signals. Derived from satellite altimetry (AVISO).

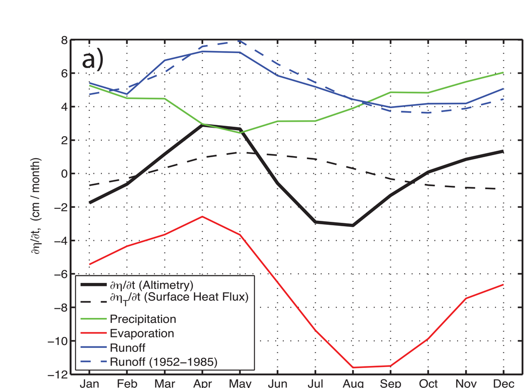

Fig. 5a The breakdown of total seasonal sea level change (**bold black**) in the Black Sea into components. Changes due to:

- surface heat flux (dashed black)
- precipitation (**green**)
- evaporation (**red**)
- due to river discharge: over the 1952-1985 period when discharge data of 5 largest rivers are available (dashed blue) and reconstructed using the Danube discharge data (**blue**)

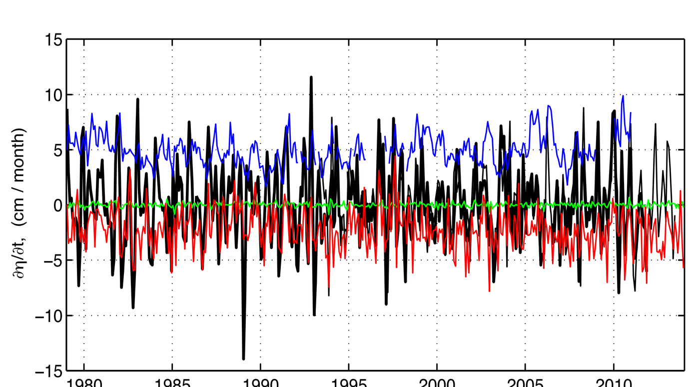

Fig. 5b Time change of non-seasonal Black Sea *SLA*: total *SLA* change inferred from the Tuapse tide gauge (**solid black**), total *SLA* change from satellite altimetry (thin black), integral *SLA* change due to precipitation and evaporation (**red**), *SLA* change due to river discharge (**blue**) and net surface heat flux (**green**).

3.2 Driving mechanisms of Sea Level variations – connections to large-scale atmospheric circulation

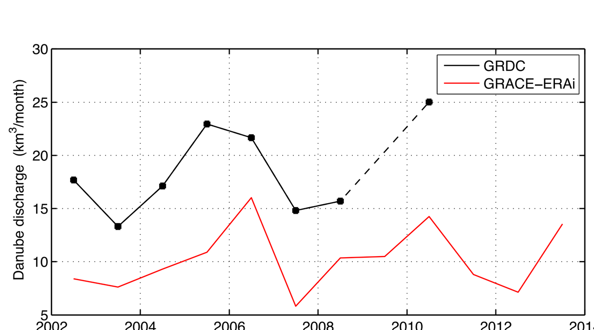

Fig. 6 Yearly Danube discharge from GRDC gauges, and from combining GRACE terrestrial water storage and ERA-I precipitation and evaporation data. Net ERA-I precipitation is strongly low-biased, but despite the bias, GRACE-ERA-I captures interannual discharge variability well.

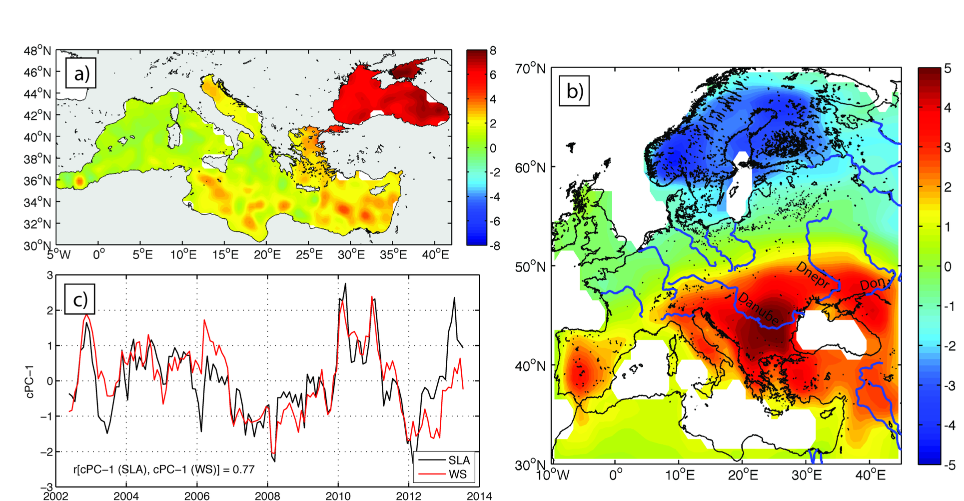

Fig. 7 Coupled EOF-1 of satellite altimetry *SLA* and GRACE water storage (*S*), shown as regression maps of (a) *SLA* and (b) *TWS* projected on (c) cPC-1 of *SLA* (**black curve**) and cPC-1 of *TWS* (**red curve**), respectively. The units are in cm per standard deviation.

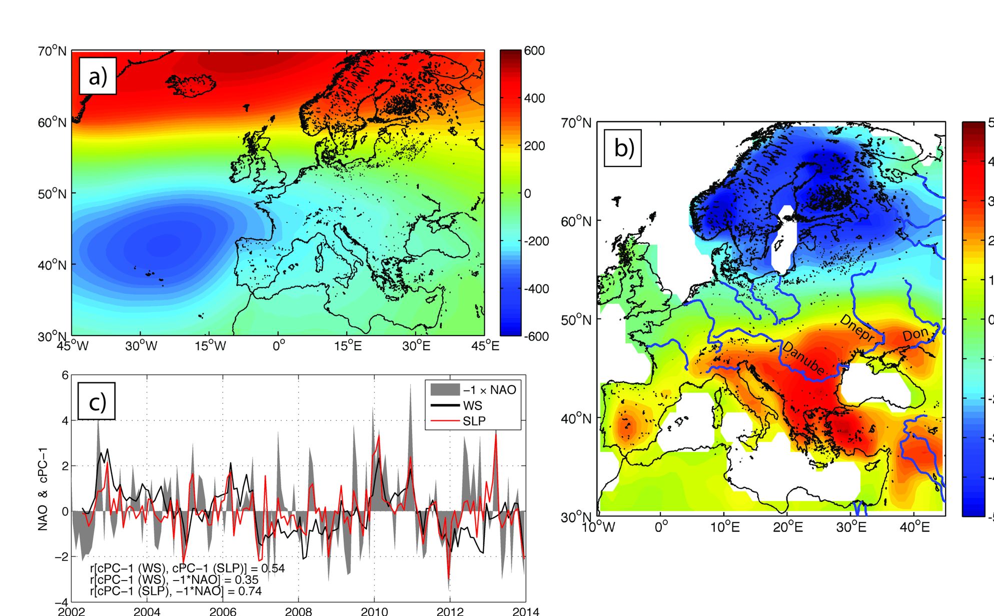

Fig. 8 Coupled EOF-1 of ERA-Interim *SLP* and GRACE TWS, shown as regression maps of (a) *SLP* and (b) *TWS* projected on (c) cPC-1 of *SLP* (red curve) and cPC-1 of *TWS* (black curve), respectively. Units: Pa per standard deviation for *SLP* and cm per standard deviation for *TWS*. NAO*-1 index shown in (c) by gray area.

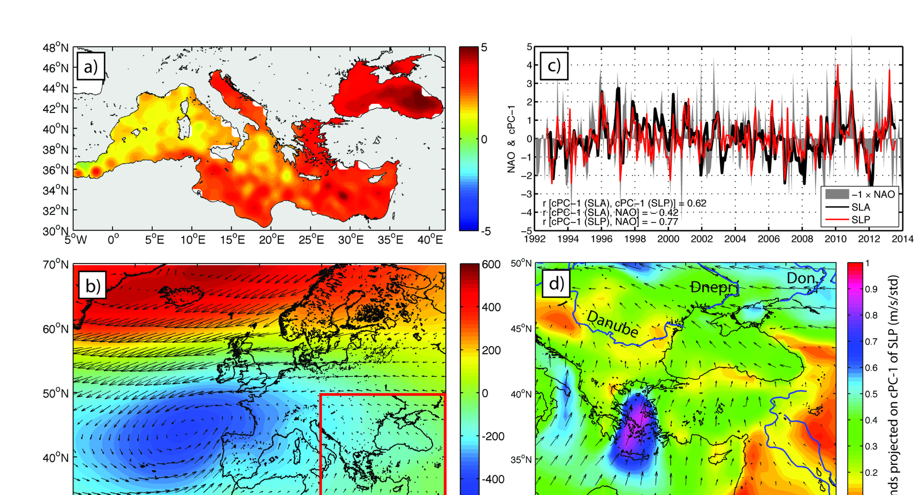

Fig. 9 Coupled EOF-1 of altimetry *SLA* and ERA-Interim *SLP*, shown as regression maps of (a) *SLA* and (b) *SLP* projected on (c) cPC-1 of *SLA* (black curve) and cPC-1 of *SLP* (red curve), respectively; NAO*-1 index shown in (c) by gray area. Regression map of the ERA-Interim winds projected on cPC-1 of *SLP* fields is shown by wind vectors in (b) and zoom-in on eastern Mediterranean and Black Sea along with absolute wind strength (d).

4. References

1. Landerer, F.W., D.L. Volkov (2013), The anatomy of recent large sea level fluctuations in the Mediterranean Sea, Geophys. Res. Lett., 40, 553–557, doi:10.1002/grl.50140.
2. Volkov, D.L., Landerer, F.W. (2014), Internal and external forcing of sea level variability in the Black Sea, Clim. Dyn., (under review).